THE EFFECT OF DIFFERENT CARBON NANOTUBE CONCENTRATION ON GLASS FIBER REINFORCED PLASTIC COUPONS UNDER PROGRESSIVE DAMAGE ACCUMULATION TESTS

Nikolaos D. Alexopoulos[a*], Ilona Lazaridou[a], Achilles Vairis[b], Markos Petousis[b]

[a] *Department of Financial Engineering, University of the Aegean, Chios, 82100, Greece*
[b] *Department of Mechanical Engineering, Crete Institute of Technology, Heraklion, 710 04, Greece*

* *nalexop@aegean.gr*

Keywords: Carbon nanotubes, Glass fibers, Mechanical properties, Electrical resistance

Abstract

GFRP plates were manufactured using Vacuum Assisted Resin Infusion (VARI) were manufactured with different geometrical dimensions and with either neat epoxy resin or doped with CNTs at various concentrations. Tensile tests were applied to GFRP specimens to seek their quasi-static mechanical properties along with their in-situ surface electrical resistance change (ERC) measurements. It has been found that the additions of specific CNT percentages quite enhance the cyclic behaviour of the coupons while other, e.g. 3 w.p. CNTs quite downgrades it. The mechanical behaviour of the coupons was examined in different testing regimes that matrix cracking, debonding and delamination are evident. Finally, the effect of measuring length is examined in the present study; for every different CNTs percentage coupon, three different measuring lengths were selected, namely 25, 75 and 125 mm to monitor the surface electrical resistance change during mechanical loading. Parameters to express the different electrical resistance measurements to gauge length, e.g. electrical resistance change divided to gauge length, are attempted and discussed in the paper. It has been shown that the lower the gauge length is, the lower the measuring ERC discrepancies are.

1. Introduction

During the last decades, there has been a strong demand increase in the aerospace sector for composite materials. Use of carbon nanotubes (CNT) in polymer composites has attracted great attention nowadays due to their excellent mechanical and electrical properties. Using resin reinforced with CNTs, a non-conductive GFRP composite can now become electrically conductive. Therefore, exploiting the methodology of Baron and Schulte [1] with the electrical resistance change of the electrically conductive CFRPs, GFRPs can now be monitored by measuring simultaneously surface electrical resistance change of a coupon during mechanical loading. Therefore, the addition of electrically conductive CNTs offers to non-conductive GFRP composites the potential for sensing capabilities through changes in electrical resistance on the onset of damage [2, 3] and enhanced fracture properties e.g. [4, 5].

Research on these newly-developed, multi-functional materials is mainly focused on the enhancement of their mechanical performance as well as measurements of electrical resistance change simultaneously recorded from stress/strain variances of the testing specimens, e.g. [5]. However, critical parameters such as the mechanical/electrical response under cyclic loadings or even fatigue are scarcely reported on the open literature.

2. Material manufacturing and experimental procedure

The resin used was a typical resin used in the aeronautics, Araldite LY 564. It was selected primarily to its low viscosity and its high mechanical properties. For each different case, resin of approximate 400 g and different percentages of carbon nanotubes were mixed in the dissolver. Use of Torrus Mill dissolver was preferred since it introduces high shear forces by a high speed rotating disc and the compound is stirred in a vacuum container to avoid air inclusions. Dissolver's mixing time of the resin with the different percentages of CNTs, namely 0.5%, 0.75% and 3.0% lasted more than 24 h each. Resin was then mixed with the catalyst (Aradur 2954 by Huntsman) and was placed on open metallic moulds and in the shape of a typical tensile specimen. Electrical cable connectors were attached in three different measuring lengths were selected, namely 25, 75 and 125 mm to the tensile specimens in order to record the electrical resistance change.

For the manufacturing of the composite plate the following process was followed: 10 plies of glass fiber fabric (style 6781, S2 glass by Fiber Glast Developments Corporation), oriented at 0/90° had been cut at the required dimensions (300 x 300 mm). The plies were laid and the wrap faces were alternated upwards and downwards during the lay-up, resulting in a cross-ply balanced and symmetric laminate. Resin with different percentages of carbon nanotubes, prepared from the previous section, was used to manufacture the composites with the same lay-up sequence. Vacuum infusion method had been used to manufacture the plates of the material. Appropriate bagging material was placed, vacuum was then applied and the infusion of the resin followed. The manufactured plates was thereafter cured for 2 hours at 60°C followed by a 4 hour at 120°C post cure, as recommended by the resin manufacturer's data sheet**.**

The tensile specimens had been cut from the material plates according to the ASTM D3039 specification and edge-polished. The dimensions of the testing specimens were width x length = 25 mm x 250 mm. Electrical cable connectors were attached to the specimen's surface. The cables were connected to the Agilent multimeter and the initial resistance of the reference test section was measured**.**

Tensile tests were applied to GFRP specimens to seek their quasi-static mechanical properties along with their in-situ surface electrical resistance change (ERC) measurements. The higher CNTs percentage in the resin matrix strongly influenced all quasi-static mechanical properties and especially modulus of elasticity and elongation to fracture. Composite coupons were also tested in progressive damage accumulation tests (PDA) to seek the composites response in quasi-static incremental cyclic loadings. The same loading protocols were applied to coupons doped with different percentages of CNTs to investigate the degradation of the different multifunctional composites under the same mechanical loadings that is well known that impose specific internal damage to the composite.

3. Result and discussion

The mechanical tensile test results of the manufactured coupons can be seen in Figure 1. It can be seen that the addition of several nanotubes increased the modulus of elasticity by approximately 5% with 1.0% wt MWCNTs (in red colour). However, a distractive point is the reduction in ductility that is approximately 40% for the same addition percentages. As the CNTs have breaking strength of the order of 0.5-1.0 TPa, they essentially increased the ultimate tensile strength of the coupons.

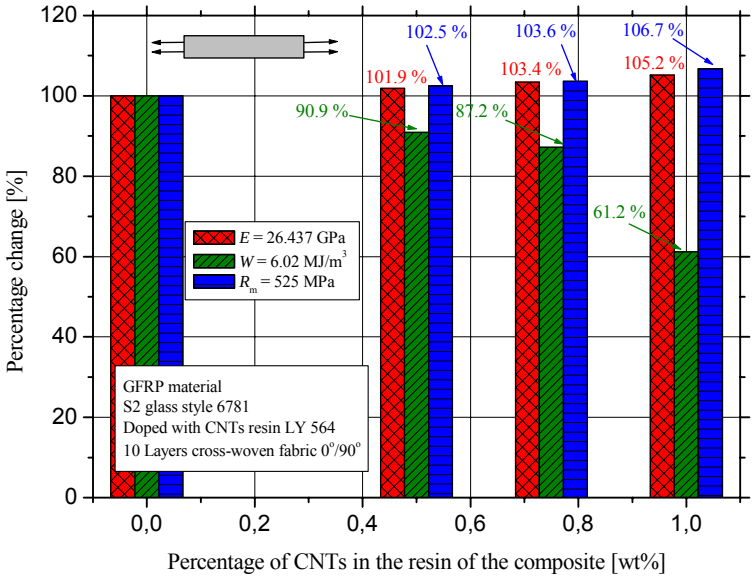

Figure 1**:** Percentage change of axial mechanical properties modulus of elasticity *E*, strain energy density *W* and tensile strength R_m due to the addition of CNTs in the resin matrix.

Progressive damage accumulation (PDA) tests had been performed in coupons with and without the CNTs reinforcement (reference). Loading – unloading steps of the PDA tests ranged from four (4) up to eleven (11). Typical axial nominal stress – strain diagrams for the eleven incremental loadings for a 0.5% wt CNTs coupon can be seen in Figure 2a. As the tests were load controlled after the unloading the specimen returned to its zero load (stress) condition. The incremental tensile loading steps of additional 50 MPa each, introduced damage to the material that can be noticed as residual strain measurements after every unloading step. Both networks of curves in the two Figures seem to be very similar. A more detailed approach to seek the differences in structural integrity of the different coupons can be assessed via introduced damage that can be expressed in these materials through stiffness degradation and residual strain measurements.

Figure 2b shows the respective electrical resistance results of the same coupon for two measuring distances, 25 mm each. As can be seen in the Figure, the two measuring gauge lengths exhibit absolutely the same resistance measurements for the first cycles. However, after the fifth cycle (approximately after 250 MPa stress) then residual resistance measurements was noticed, that evolved differently for the two gauge lengths. As can be seen in Figure 3, final fracture of the coupons occurred inside the b measuring length that explains the in principal higher recorded resistance measurements as well as the higher residual resistance measurements after mechanical unloading.

Damage develops to the composite with the incremental, quasi-static loading – unloading steps. Depending on the magnitude of the peak load value, different kind of damage is developed to the composite, e.g. for the low loading values, mainly matrix cracking and debonding between matrix and fibers happens; for medium loading values delamination

occurs, while for loadings close to the ultimate tensile load, the main damage mechanism is fibre breakage. Location of the development of damage is strictly linked with the main damage mechanism of the composite. Briefly, with increasing loading, location of the damage occurs firstly in the matrix, then to the interface between the plies of the composite and the final step is the failure of the fibres.

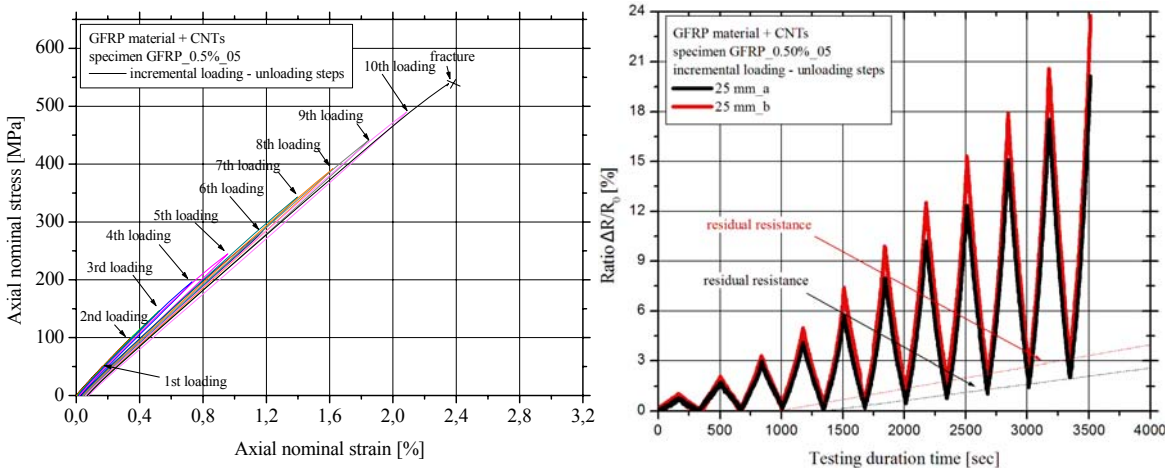

Figure 2**:** (a) Nominal stress – strain curves for different loading – unloading steps of GFRP with 0.5%wt CNTs coupon and (b) typical electrical resistance change for the same coupon under the same loading protocol.

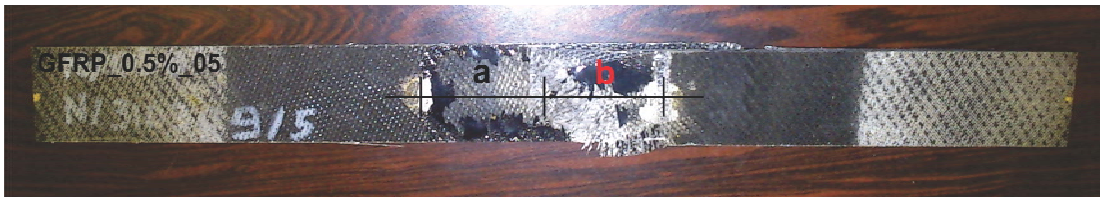

Figure 3: Fracture occurred to the b measuring gauge length of the coupon.

Despite that the damage mechanisms are well known, there is no absolute measure amongst researchers to quantify damage. Pantelakis et al. used ultrasonics to quantify the developed damage in APC2 composites after fatigue testing [6] and correlate the findings with residual mechanical properties of the material. Loutas and Kostopoulos used acousto-ultrasonics and acoustic emission techniques to quantify damage development in carbon/carbon, woven reinforced composites [7]. Philippidis et al. classified acoustic emission signals from composites as to their origin in order to characterize each individual damage mechanism [8]. Recently, Aggelis et al. characterized the transition of the damage mechanism from transverse matrix cracking to delamination in cross-ply laminates using advanced AE indices [9]. Nevertheless, from the mechanical point of view, developed damage to the composite can be calculated by the reduction of the modulus of elasticity or by the normalized modulus of elasticity E/E_0.

Figure 5 shows the decrease of the normalized modulus of elasticity for a number of coupons with incremental tensile loading steps. The test results for the coupons without and with CNTs can be seen in the Figure, as well as the main damage mechanisms of the investigated composite. Stiffness decrease is almost the same for the specimens with and without CNTs. The stiffness degradation follows the same pattern regardless the presence or the concentration of the CNTs. An exception seems to be the 0.75% concentration, where lower normalized modulus of elasticity decrease was noticed that implies better cyclic mechanical performance. Additionally, fracture of the specimens always initiated and occurred within the gauge length of the coupon.

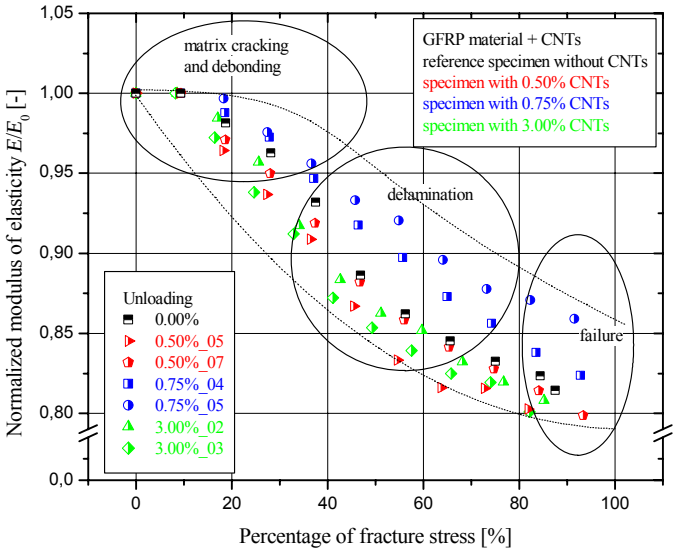

Figure 4**:** Modulus of elasticity degradation due to progressive damage accumulation tests in coupons.

Typical mechanical strain – electrical resistance change diagram for 0.50% wp CNTs can be seen in Figure 5 for the 11 different steps till fracture. Each loading maxima is marked in the Figure, where a hysteresis loop is formed for all cases after unloading. Loading branch of each step follows always an exponential curve while unloading branch seems to be linear. Besides the expected residual strain measurements after every unloading step, noticeable is also the residual resistance change measurements. Essential residual resistance measurement is recorded, with a maximum value of approximate 3 % at the last loading step.

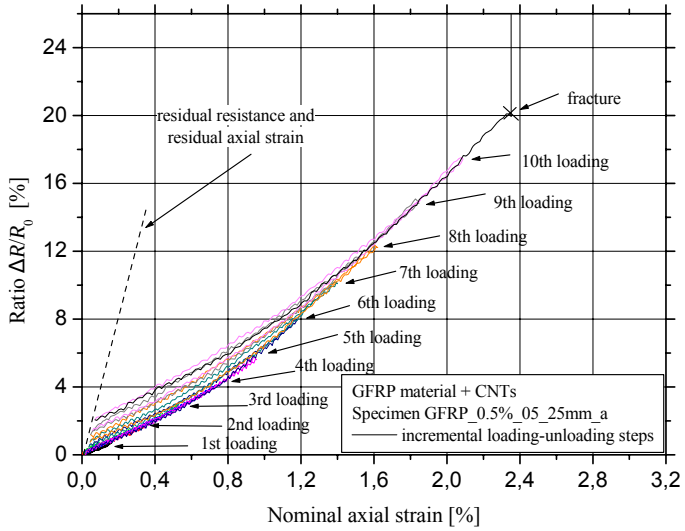

Figure 5: Typical resistance versus strain measurements of increasing loading – unloading tests for the coupon with 0.50% wp CNTs

A typical eleven incremental loading – unloading loops can be seen in Figure 7 for all investigated coupons reinforced with CNTs in the resin. In the plots, electrical resistance change of the coupon can be seen for all different maximum loading levels and returning to zero state. At higher stresses exceeding 250 MPa (fifth cycle), essential damage occurred to the composite due to mechanical loading, since a hysteresis loop was formed for the resistance change measurements. This hysteresis loop formation was even further noticeable for the higher incremental loading – unloading steps of the composite. Noticeable is also that the resistance change after every unloading does not return to its initial value. Residual

resistance change measurements were recorded for all coupons. Especially for the larger CNT concentration (3.0% wp CNTs), an inverse phenomenon was observed, that resistance change was decreasing, calculating also negative electrical resistance change values. Such tests were continuously repeated to other coupons with the same concentration and absolutely the effect was observed. Negative ERC values after unloading means that with the mechanical loading the vast population of CNTs are coming together, resulting in more CNT contacts that decrease electrical resistance. Nevertheless, observed residual resistance after every unloading step should be considered as a measure of induced damage to the composite due to mechanical loading.

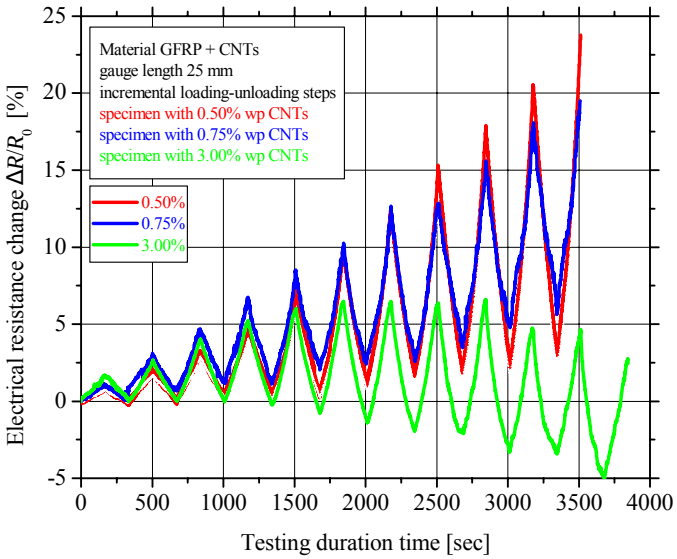

Figure 6: Typical electrical resistance change of specimen with different percentages of CNTs

Figure 7 shows the electrical resistance change results of 0.75% wp CNTs for the same loading protocol and for different measuring distances (gauge length), namely 25, 75 and 125 mm. It can be seen that the smaller gauge length gave the lowest discrepancies from all investigated lengths. Again, residual resistance change was noticed for every single gauge length, with an increasing trend after the cumulative loading cycles.

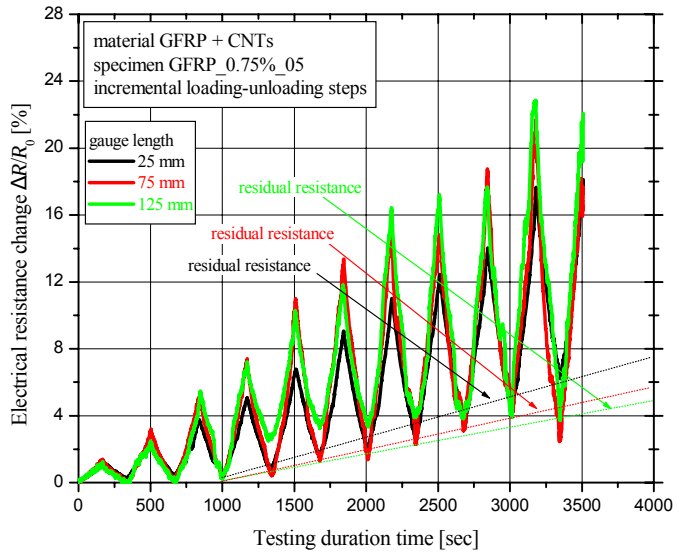

Figure 7: Electrical resistance change of GFRP+0.75%wp CNTs over typical loading cycle and for different measuring gauge lengths

Figure 8 shows the electrical resistance plots over the seventh loading – unloading cycle. This cycle corresponds to 0 – 350 – 0 MPa loading cycle that is well above the 50% of ultimate fracture stress of the composite. Hence, matrix cracking is evident form previous loadings as well as debonding and delamination. The resistance data were selected to be plotted over the following three cases: (a) resistance change over measuring length ($\Delta R/L$), (b) resistance change over initial resistance ($\Delta R/R_0$) and finally (c) resistance change over initial resistance and measuring length ($\Delta R/R_0 L$). The results of the calculations can be seen in Figure 8 over three different measuring lengths, namely 25, 75 and 125 mm. It can be seen that Figure 8a and b gives almost quantitative same results in terms of the hysteresis loops as well as the peak calculated values. Maximum peak values were calculated for the higher gauge lengths, namely the 125 mm. On the contrary, Figure 8c shows the complete opposite trend, with the lowest gauge length having the highest calculated values at peak loading; the aim when conceiving ratio ($\Delta R/R_0 L$) was to quantify in the same ratio the initial resistance value as well as measuring length that seems to affect the calculations.

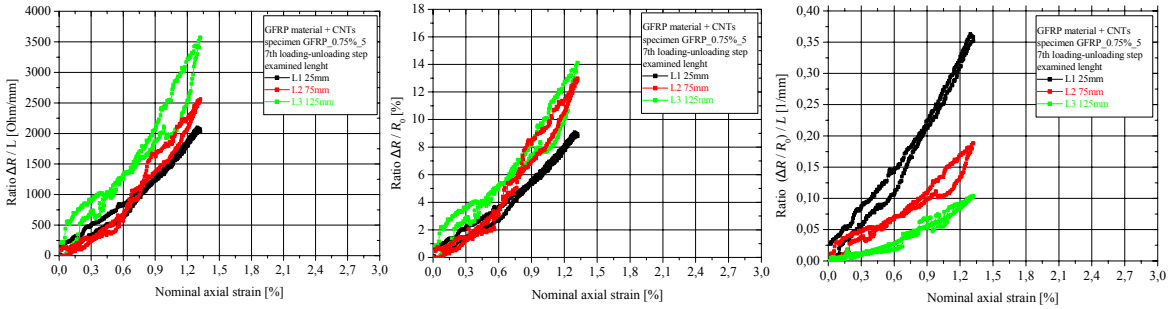

(a) (b) (c)

Figure 8: Calculation plots of the seventh loading loop over GFRP+0.75%wp CNTs and for various measuring gauge lengths

Acknowledgments

The authors gratefully acknowledge the financial support of the "NANOSTRENGTH" Project (Archimedes Framework) of the Crete Institute of Technology, which is co-financed by Greece and the European Union under the hospices of the program "Education and lifelong learning investing in knowledge society". Ministry of Education and religious affairs, culture and sports, NSRF 2007-2013.

References

[1] K. Schulte and Ch. Baron. Load and failure analyses of CFRP laminates by means of electrical resistivity measurements. *Composites Science & Technology*, 36: 349-356, 1989.

[2] E.T. Thostenson and T.W. Chou. Carbon Nanotube Networks: Sensing of Distributed Strain and Damage for Life Prediction and Self Healing. *Advanced Materials*, 18: 2837-2841, 2006.

[3] E.T. Thostenson and T.W. Chou. Real-Time in situ Sensing of Damage Evolution in Advanced Fiber Composites using Carbon Nanotube Networks. *Nanotechnology*, 19**:** 215713, 2008.

[4] L. Boeger, MHG Wichman, L.O. Meyer and K. Schulte. Load and health monitoring in glass fibre reinforced composites with an electrically conductive nanocomposite epoxy matrix. *Composites Science & Technology*, 68: 1886-1894, 2008.

[5] MHG Wichman, S.T. Buschhorn, L. Boeger, R. Adelung and K. Schulte. Direction sensitive bending sensors based on multi-wall carbon nanotube/epoxy nanocomposites. *Nanotechnology*, 19, 475, 2008.
[6] Sp.G. Pantelakis, E.C. Kyriakakis and P. Papanikos. Non-destructive fatigue damage characterization of laminated thermosetting fibrous composites. *Fatigue and Fracture of Engineering Materials and Structures*, 24 (10): 651-662, 2001.
[7] T.H. Loutas and V. Kostopoulos. Health monitoring of carbon/carbon, woven reinforced composites. Damage assessment by using advanced signal processing techniques. Part I: Acoustic emission monitoring and damage mechanisms evolution. *Composites Science & Technology*, 69 (2): 265-272, 2009.
[8] T.P. Philippidis and T.T. Assimakopoulou. Using acoustic emission to assess shear strength degradation in FRP composites due to constant and variable amplitude fatigue loading. *Composites Science & Technology*, 68 (15-16): 3272-3277, 2008.
[9] D.G. Aggelis, N.M. Barkoula, T.E. Matikas and A.S. Paipetis. Acoustic emission monitoring of degradation of cross ply laminates. *Journal of the Acoustical Society of America*. 127 (6): 246-251, 2010.